

(Z)-4,4'-Stilbene dicarboxylic acid, the overlooked metal-organic framework linker. †

Lucy R. Hunter,^{*a} Joshua. K.G. Karlsson,^a Jonathan. D. Sellars,^{b,c} Michael. R. Probert.^{*a}

a- Department of Chemistry, School of Natural and Environmental Sciences, Newcastle University, Newcastle upon Tyne, NE1 7RU, UK

b- Biosciences Institute, Faculty of Medical Sciences, Newcastle University, Newcastle upon Tyne NE2 4HH, UK

c- School of Pharmacy, Faculty of Medical Sciences, King George VI Building, Newcastle upon Tyne NE1 7RU, UK

Supplementary information

Contents

1. Crystallographic information files (CIF)
2. Materials and methods
 - 2.1 General remarks
 - 2.2 Single crystal x-ray diffraction
 - 2.3 Synthesis
3. Fourier-transform infrared spectroscopy (FT-IR)
4. Thermogravimetric analysis (TGA) and differential scanning calorimetry (DSC)
5. Powder x-ray diffraction (PXRD)
6. Luminescence data

Table S1: Crystallographic data for frameworks 1-5, measured using either a Bruker D8 venture or XtaLAB Synergy at 150K, e.s.d.s (). (L) = SDC

Identification code	2D Sm (1)	2D Eu (2)	2D Gd (3)	2D Tb (4)	2D Ho (5)
Empirical formula	$C_{79}H_{85}N_5O_{25}S$	$C_{79}H_{85}Eu_2N_5$	$C_{76}H_{78}Gd_2N_4$	$C_{79}H_{85}N_5O_{25}$	$C_{79}H_{85}Ho_2N_5$
Formula weight	1805.21	1808.43	1745.92	1822.35	1834.37
Temperature/K	150.00(10)	149.99(10)	150.00	149.99(10)	150.00
Crystal system	triclinic	triclinic	triclinic	triclinic	triclinic
Space group	P-1	P-1	P-1	P-1	P-1
a/Å	9.65620(10)	9.64310(10)	9.6431(7)	9.62980(10)	9.6157(9)
b/Å	11.69050(10)	11.66930(10)	11.6865(9)	11.64840(10)	11.6530(11)
c/Å	35.0640(4)	34.9873(4)	34.943(3)	35.0490(4)	34.944(3)
α /°	91.2650(10)	91.2120(10)	90.941(3)	91.2880(10)	91.143(3)
β /°	93.9650(10)	93.9490(10)	94.270(3)	94.1520(10)	94.270(3)
γ /°	93.6030(10)	93.5860(10)	93.617(4)	93.7930(10)	93.785(4)
Volume/Å ³	3939.56(7)	3918.74(7)	3918.2(5)	3911.13(7)	3894.9(6)
Z	2	2	2	2	2
ρ calcg/cm ³	1.522	1.533	1.480	1.547	1.564
μ /mm ¹	1.557	1.667	11.478	1.875	4.366
F(000)	1836.0	1840.0	1764.0	1848.0	1856.0
Crystal size/mm ³	0.23 × 0.15 × 0.11	0.225 × 0.083 × 0.022	0.9 × 0.3 × 0.05	0.22 × 0.14 × 0.05	0.13 × 0.11 × 0.03
Radiation	Mo K α (λ = 0.71073)	Mo K α (λ = 0.71073)	Cu K α (λ = 1.54178)	Mo K α (λ = 0.71073)	Cu K α (λ = 1.54178)
2 θ range for data collection/°	3.71 to 51.362	4.156 to 60.936	5.074 to 144.906	4.156 to 60.542	5.074 to 133.774
Index ranges	-11 ≤ h ≤ 11, -14 ≤ k ≤ 13, -42 ≤ l ≤ 42	-12 ≤ h ≤ 12, -14 ≤ k ≤ 15, -46 ≤ l ≤ 48	-11 ≤ h ≤ 11, -14 ≤ k ≤ 14, -43 ≤ l ≤ 43	-13 ≤ h ≤ 12, -16 ≤ k ≤ 13, -47 ≤ l ≤ 44	-11 ≤ h ≤ 11, -13 ≤ k ≤ 13, -41 ≤ l ≤ 41
Reflections collected	61624	49714	50879	60341	54631
Independent reflections	14946 [R _{int} = 0.0324, R _{sigma} = 0.0288]	18912 [R _{int} = 0.0383, R _{sigma} = 0.0491]	15046 [R _{int} = 0.0644, R _{sigma} = 0.0597]	19273 [R _{int} = 0.0323, R _{sigma} = 0.0385]	13589 [R _{int} = 0.0540, R _{sigma} = 0.0458]
Data/restraints/parameters	14946/808/1028	18912/808/1028	15046/777/971	19273/801/1018	13589/801/1018
Goodness-of-fit on F ²	1.037	1.030	1.084	1.040	1.044
Final R indexes [I > 2 σ (I)]	R ₁ = 0.0229, wR ₂ = 0.0503	R ₁ = 0.0320, wR ₂ = 0.0666	R ₁ = 0.0509, wR ₂ = 0.1354	R ₁ = 0.0281, wR ₂ = 0.0607	R ₁ = 0.0391, wR ₂ = 0.0991
Final R indexes [all data]	R ₁ = 0.0282, wR ₂ = 0.0524	R ₁ = 0.0479, wR ₂ = 0.0717	R ₁ = 0.0580, wR ₂ = 0.1412	R ₁ = 0.0383, wR ₂ = 0.0642	R ₁ = 0.0430, wR ₂ = 0.1020
Largest diff. peak/hole / e Å ⁻³	0.46/-0.40	1.00/-0.49	1.75/-1.55	1.75/-0.66	1.86/-0.53

Table 2: Crystallographic data for frameworks 6-10, measured using a Bruker D8 venture 150K, e.s.d.s (). (L) = SDC

Identification code	3D Eu (6)	3D Gd (7)	3D Tb (8)	3D Ho (9)	3D Er (10)
Empirical formula	$C_{60}H_{64}Eu_2N_4O_{19}$	$C_{54}H_{50}Gd_2N_2O_{17}$	$C_{60}H_{64}N_4O_{19}Tb_2$	$C_{60}H_{64}Ho_2N_4O_{19}$	$C_{54}H_{50}Er_2N_2O_{17}$
Formula weight	1449.07	1313.46	1462.99	1475.01	1333.48
Temperature/K	150.00	150.01	150.00	150.0	150.0
Crystal system	triclinic	triclinic	triclinic	triclinic	triclinic
Space group	P-1	P-1	P-1	P-1	P-1
a/Å	9.8652(7)	9.7244(6)	9.8353(10)	9.8235(6)	9.6965(6)
b/Å	13.8653(10)	13.8269(8)	13.8578(13)	13.8714(9)	13.7603(9)
c/Å	22.5242(16)	22.6816(14)	22.505(2)	22.4913(15)	22.5832(14)
α /°	83.601(4)	83.161(4)	83.589(4)	83.593(3)	83.287(2)
β /°	78.971(4)	79.170(4)	78.689(4)	78.224(3)	78.791(2)
γ /°	85.080(4)	84.514(4)	84.942(4)	84.961(4)	84.572(2)
Volume/Å ³	2998.6(4)	2965.7(3)	2982.0(5)	2974.9(3)	2927.5(3)
Z	2	2	2	2	2
ρ_{calc}/cm^3	1.605	1.471	1.629	1.647	1.513
μ/mm	15.467	14.863	12.160	5.466	5.725
F(000)	1460.0	1304.0	1468.0	1476.0	1320.0
Crystal size/mm ³	0.04 × 0.03 × 0.01	0.04 × 0.03 × 0.02	0.12 × 0.1 × 0.06	0.12 × 0.1 × 0.1	0.15 × 0.12 × 0.1
Radiation	CuK α (λ = 1.54178)				
2 θ range for data collection/°	6.428 to 144.72	6.456 to 133.492	6.432 to 145.576	6.426 to 145.89	6.486 to 144.628
Index ranges	-11 ≤ h ≤ 11, -17 ≤ k ≤ 16, -27 ≤ l ≤ 27	-11 ≤ h ≤ 11, -16 ≤ k ≤ 16, -26 ≤ l ≤ 26	-11 ≤ h ≤ 11, -17 ≤ k ≤ 17, -27 ≤ l ≤ 27	-12 ≤ h ≤ 11, -17 ≤ k ≤ 17, -27 ≤ l ≤ 27	-11 ≤ h ≤ 11, -16 ≤ k ≤ 16, -27 ≤ l ≤ 27
Reflections collected	92491	48013	100683	114023	128202
Independent reflections	11397 [R _{int} = 0.0827, R _{sigma} = 0.0445]	10369 [R _{int} = 0.0952, R _{sigma} = 0.0725]	11426 [R _{int} = 0.0766, R _{sigma} = 0.0392]	11480 [R _{int} = 0.0627, R _{sigma} = 0.0313]	11247 [R _{int} = 0.0642, R _{sigma} = 0.0285]
Data/restraints/parameters	11397/610/781	10369/562/683	11426/612/782	11480/612/779	11247/562/683
Goodness-of-fit on F ²	1.108	1.045	1.220	1.049	1.084
Final R indexes [I ≥ 2 σ (I)]	R ₁ = 0.0565, wR ₂ = 0.1396	R ₁ = 0.0554, wR ₂ = 0.1464	R ₁ = 0.0698, wR ₂ = 0.2064	R ₁ = 0.0552, wR ₂ = 0.1269	R ₁ = 0.0414, wR ₂ = 0.1098

Final R indexes [all data]	$R_1 = 0.0658,$ $wR_2 = 0.1449$	$R1 = 0.0699,$ $wR2 = 0.1564$	$R_1 = 0.0758,$ $wR_2 = 0.2158$	$R1 = 0.0657,$ $wR2 = 0.1344$	$R1 = 0.0445,$ $wR2 = 0.1132$
Largest diff. peak/hole / e Å⁻³	1.18/-1.35	1.69/-1.17	1.50/-1.93	1.40/-0.78	1.45/-1.66

2. Materials and methods

2.1 General remarks

(Z)-4,4'-Stilbenedicarboxylic acid, N,N-Dimethylformamide (DMF) and all lanthanide salts were used as supplied unless otherwise stated. Infrared spectra were recorded using a Diamond ATR (attenuated total reflection) accessory (Golden Gate).

Steady-state fluorescence data were collected using a Hitachi F-4500 spectrophotometer where solid samples were sandwiched between a microscope slide and a coverslip and mounted on an adjustable stage so that emission could be detected off the surface of the samples at a shallow angle of approximately 30°. Fluorescence lifetime measurements were obtained using a PTI EasyLife 2 system where excitation was with a 305 nm diode laser.

Thermogravimetric analysis (TGA) was performed using Netzsch STA Jupiter simultaneous TGA-DSC system, heating rate 10 °C per minute. Powder X-ray diffraction (PXRD) measurements were conducted using a XRD3 – Bruker D2 Phaser with CuK α radiation.

2.2. Single-crystal X-ray diffraction

Suitable single crystals of **3,5**, and **6-10** were grown as described and for analysis were collected on a Bruker D8 Venture diffractometer using a CuK α I μ S X-radiation source ($\lambda = 1.5406 \text{ \AA}$), and a Photon II detector. The single crystals were maintained at 150 K during data collections using an Oxford Cryosystems cryostream. Data collection and reduction were carried out using APEX III software interface, before final post processing and absorption scaling with SADABS.¹ Structures were solved and refined using the Olex2 interface² to the ShelX suite of programs, XT for structure solution and XL for structure refinement.^{3,4}

Suitable single crystals of frameworks **1,2** and **4** were grown as described and for analysis were collected on a Rigaku XtaLAB Synergy using a MoK α Dualflex radiation source and a HyPix-Arc 100 detector. The single crystals were maintained at 150 K during data collections using an Oxford Cryosystems cryostream. Data collection and reduction were carried out using CrysAlis Pro software CCD and RED interface.⁵ Structures were solved and refined using the Olex2 interface² to the ShelX suite of programs, XT for structure solution and XL for structure refinement.^{3,4}

2.3 Synthesis and characterisation of frameworks

Compounds **1-10** were synthesised using evaporative crystallisation following the general procedure outlined:

(Z)-4,4'-stilbene dicarboxylic acid (20 mg, 75 μ mol) and the appropriate lanthanide salt (1.2 equiv.) were added to a glass vial. N,N-Dimethylformamide (2 mL) was then added to the mixture and subsequently heated at 100 °C for 2h. Any remaining solid was filtered and the filtrate decanted into another glass vial and left to evaporate in a vented cupboard for up to 20 weeks.

2D Coordination polymers

Sm₂((Z)-SDC)₆(H₂O)₄ (1): Complex **1** was synthesised following the general procedure above using SmCl₃.xH₂O yielding cream plate crystals after 4 weeks. (C₆₄H₄₈O₂₀Sm₂) (M_w = 1439.79 g/mol): Selected FTIR (cm⁻¹) 789 (m), 1406 (s), 1523 (s), 3290 (b).

Eu₂((Z)-SDC)₆(H₂O)₄ (2): Complex **2** was synthesised following the general procedure above using EuCl₃.xH₂O yielding colourless plate crystals after 8 weeks. (C₆₄H₄₈O₂₀Eu₂) (M_w = 1443.00 g/mol): Selected FTIR (cm⁻¹) 726 (m), 1404 (s), 1515 (m), 3335 (b).

Gd₂((Z)-SDC)₆(H₂O)₄ (3): Complex **3** was synthesised following the general procedure above using GdCl₃.xH₂O yielding white plate crystals after 2 weeks. (C₆₄H₄₈O₂₀Gd₂) (M_w = 1453.57 g/mol): Selected FTIR (cm⁻¹) 790 (m), 1405 (s), 1520 (m), 3291 (b).

Tb₂((Z)-SDC)₆(H₂O)₄ (4): Complex **4** was synthesised following the general procedure above using TbCl₃.xH₂O yielding white plate crystals after 2 weeks. (C₆₄H₄₈O₂₀Tb₂) (M_w= 1456.92 g/mol): Selected FTIR (cm⁻¹) 1386 (s), 1651 (s), 3315 (b).

Ho₂((Z)-SDC)₆(H₂O)₄ (5): Complex **5** was synthesised following the general procedure using anhydrous HoCl₃ yielded pale yellow plate crystals after 8 weeks. (C₆₄H₄₈O₂₀Ho₂) (M_w = 1468.93 g/mol): Selected FTIR (cm⁻¹) 793 (m), 1408 (s), 1605 (m), 3217 (b).

3D MOFs

Eu₂((Z)-SDC)₃(H₂O)₂(DMF) (6): Complex **6** was synthesised following the general procedure above using EuCl₃.xH₂O yielding colourless plate crystals after 14 weeks. (C₅₁H₄₃N₁O₁₆Eu₂) (M_w = 1229.81 g/mol): Selected FTIR (cm⁻¹) 726 (m), 1404 (s), 1515 (m), 3335 (b).

Gd₂((Z)-SDC)₃(H₂O)₂(DMF) (7): Complex **7** was synthesised following the general procedure above using GdCl₃.xH₂O yielded white plate crystals after 16 weeks. (C₅₁H₄₃N₁O₁₆Gd₂) (M_w = 1240.38 g/mol): Selected FTIR (cm⁻¹) 726 (m), 1405 (s), 1517 (m), 1651 (m), 3324 (b).

Tb₂((Z)-SDC)₃(H₂O)₂(DMF) (8): Complex **8** was synthesised following the general procedure above using TbCl₃.xH₂O yielding white plate crystals after 16 weeks. (C₅₁H₄₃N₁O₁₆Tb₂) (M_w = 1243.73 g/mol): Selected FTIR (cm⁻¹) 726 (m), 1101 (m) 1384(s), 1647 (s), 3347 (b).

Ho₂((Z)-SDC)₃(H₂O)₂(DMF) (9): Complex **9** was synthesised following the general procedure above using HoCl₃.xH₂O yielding yellow plate crystals after 12 weeks. (C₅₁H₄₃N₁O₁₆Ho₂) (M_w = 1255.74 g/mol): Selected FTIR (cm⁻¹) 1386 (s), 1651 (s), 3249 (b).

Er₂((Z)-SDC)₃(H₂O)₂(DMF) (10): Complex **10** was synthesised following the general procedure above using ErCl₃.xH₂O yielded pale pink plate crystals after 16 weeks. (C₅₁H₄₃N₁O₁₆Er₂) (M_w = 1260.40 g/mol): Selected FTIR (cm⁻¹) 726 (m), 1409 (s), 1520 (m), 1662 (m), 3335 (b).

3. FT-IR

(Z)-H₂SDC

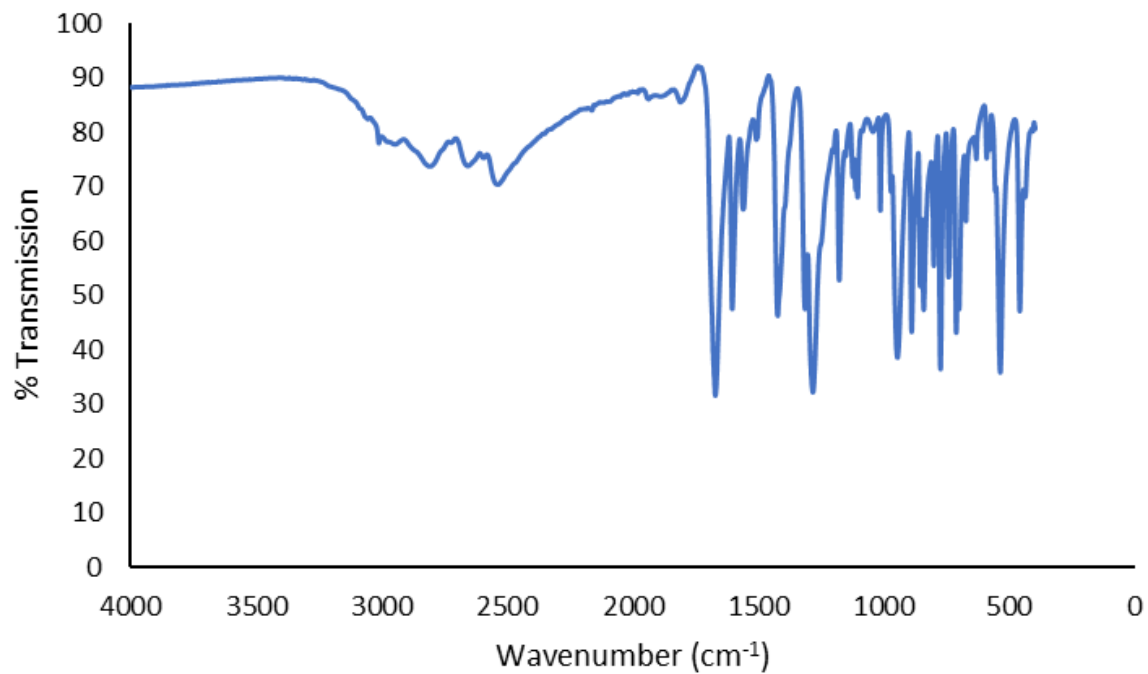


Figure S1: FTIR data for (Z)-H₂SDC. Infrared spectra were recorded using a Diamond ATR (attenuated total reflection) accessory (Golden Gate) at room temperature.

CP 1

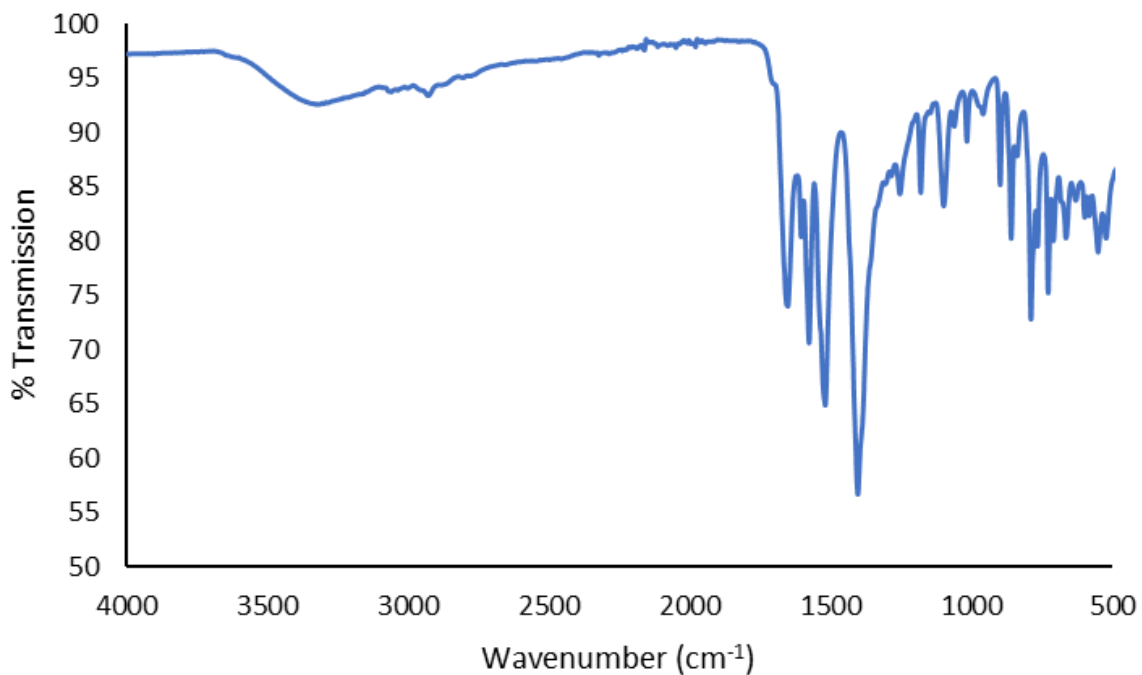


Figure S1: FTIR data for CP 1. Infrared spectra were recorded using a Diamond ATR (attenuated total reflection) accessory (Golden Gate) at room temperature.

CP 2

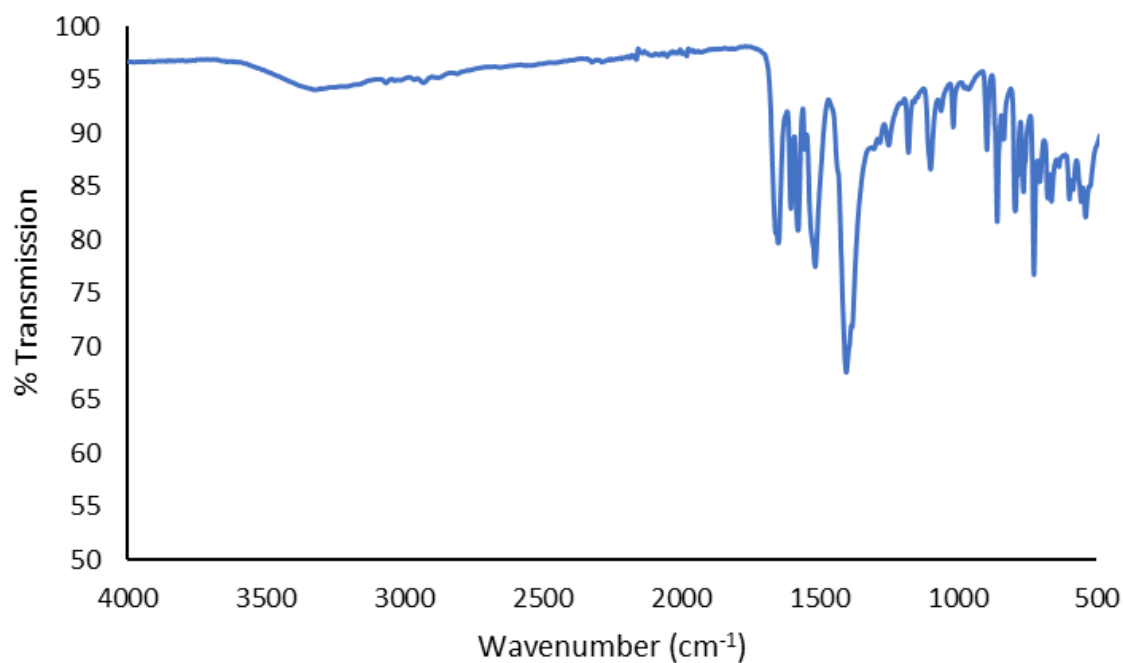


Figure S2: FTIR data for CP 2. Infrared spectra were recorded using a Diamond ATR (attenuated total reflection) accessory (Golden Gate) at room temperature.

CP 3

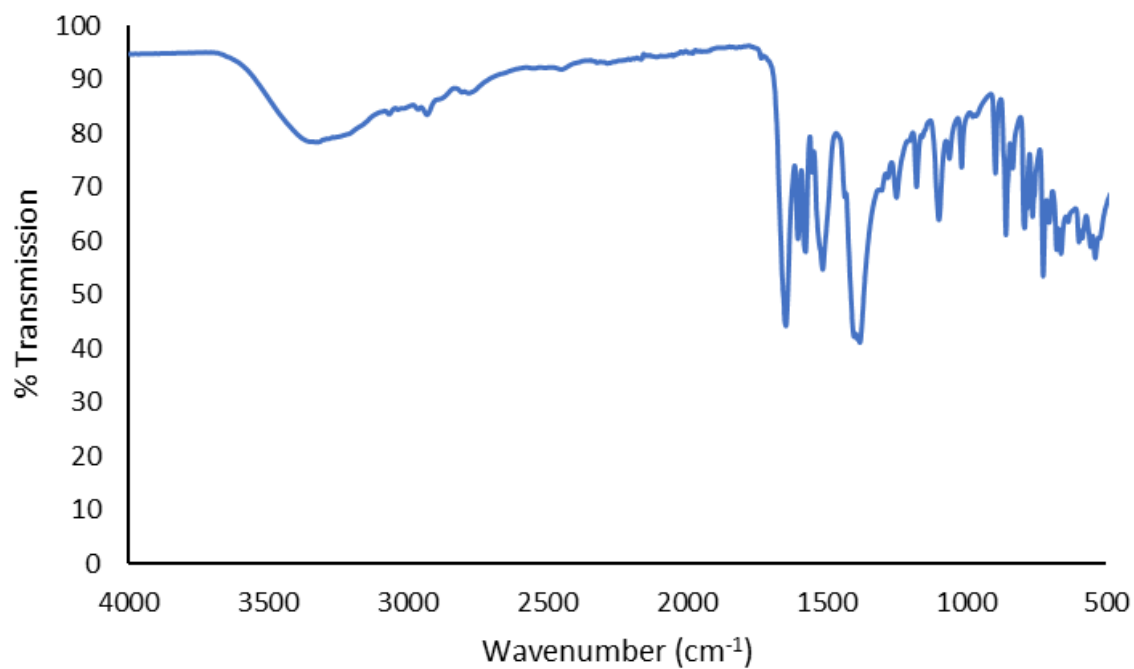


Figure S3: FTIR data for CP 3. Infrared spectra were recorded using a Diamond ATR (attenuated total reflection) accessory (Golden Gate) at room temperature.

CP 4

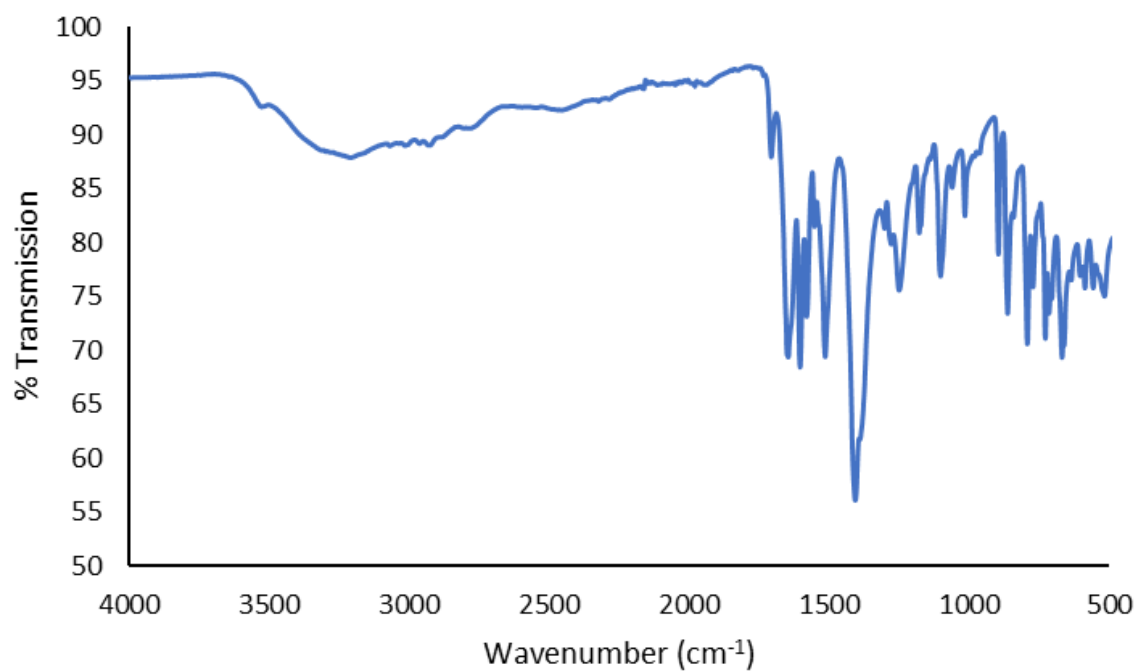


Figure S4: FTIR data for CP 4. Infrared spectra were recorded using a Diamond ATR (attenuated total reflection) accessory (Golden Gate) at room temperature.

CP 5

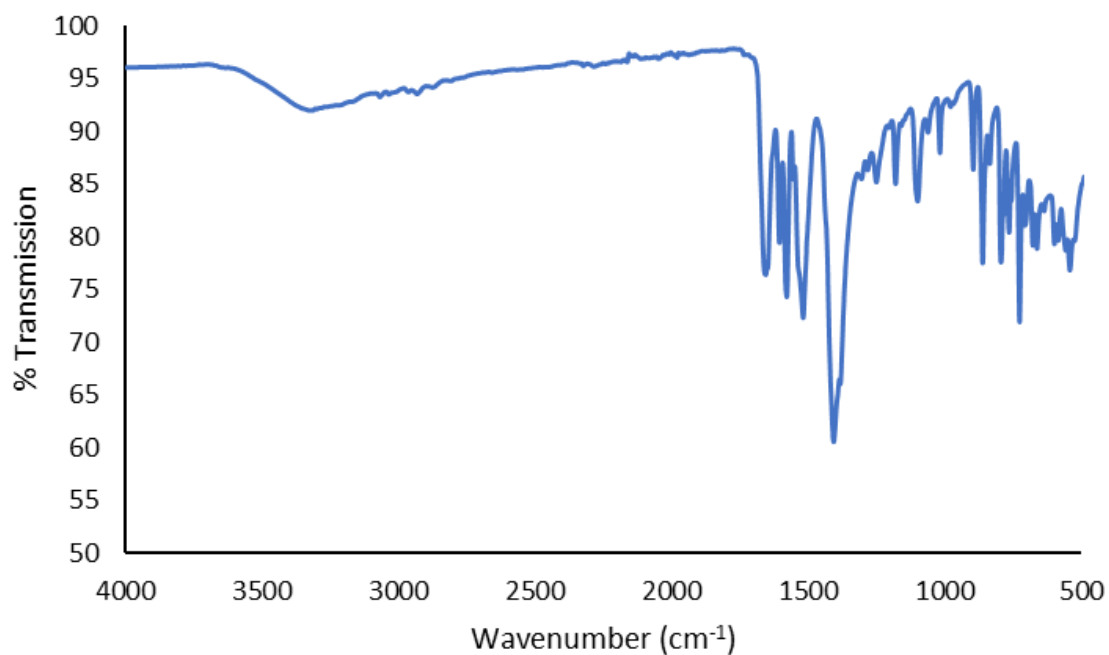


Figure S5: FTIR data for CP 5. Infrared spectra were recorded using a Diamond ATR (attenuated total reflection) accessory (Golden Gate) at room temperature.

MOF 6

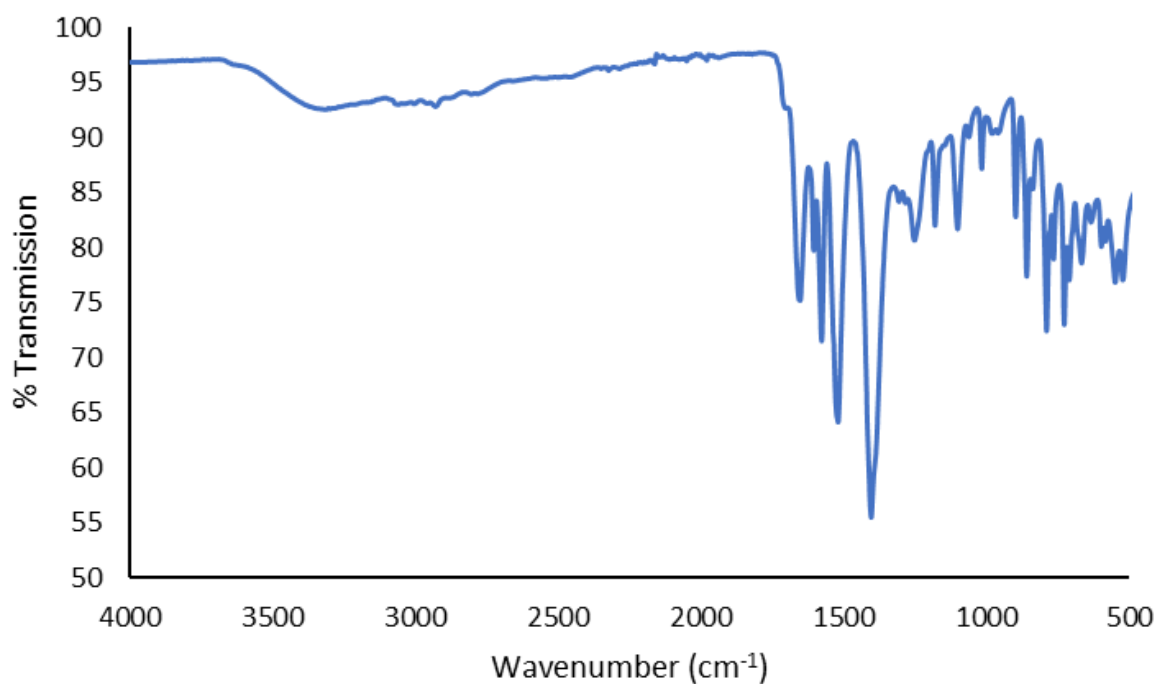


Figure S6: FTIR data for MOF 6. Infrared spectra were recorded using a Diamond ATR (attenuated total reflection) accessory (Golden Gate) at room temperature.

MOF 7

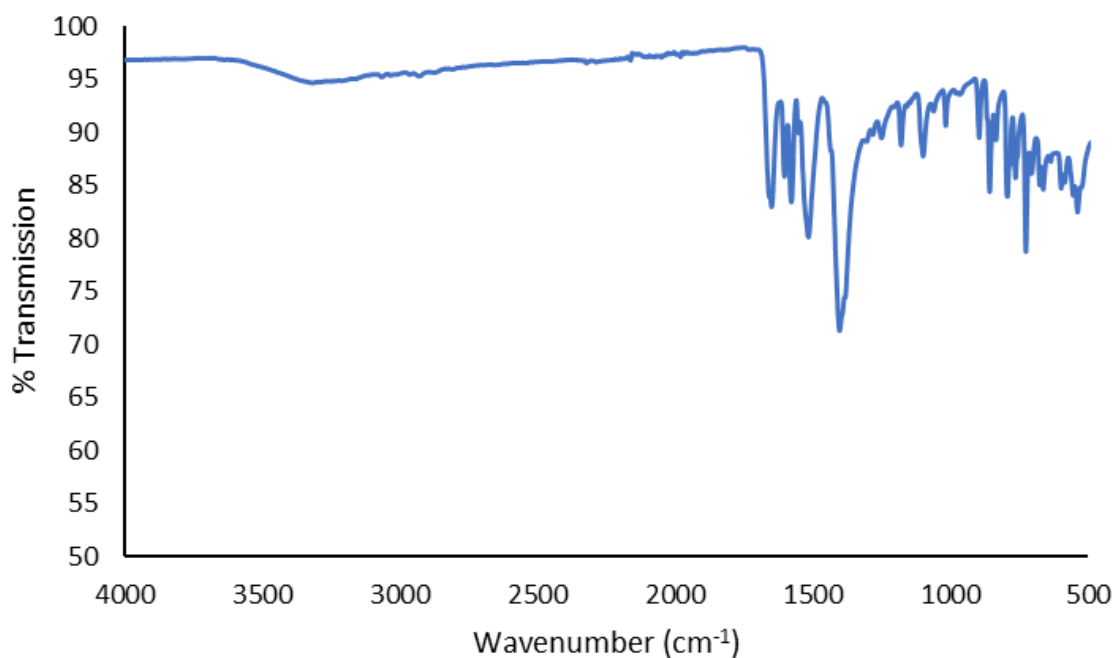


Figure S7: FTIR data for MOF 7. Infrared spectra were recorded using a Diamond ATR (attenuated total reflection) accessory (Golden Gate) at room temperature.

MOF 8

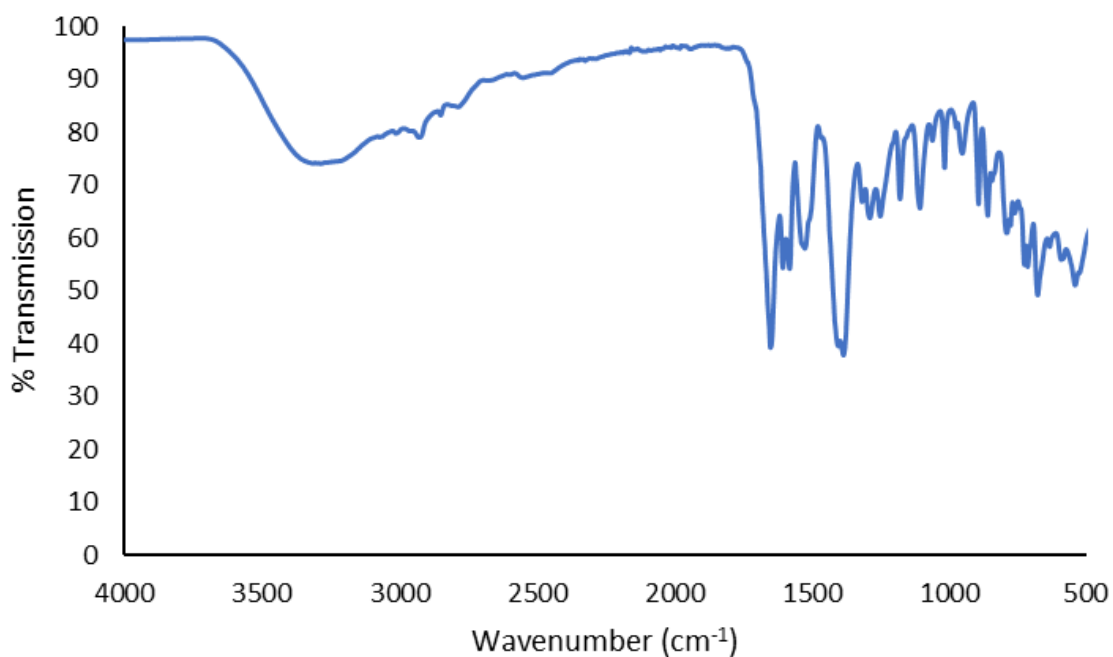


Figure S8: FTIR data for MOF 8. Infrared spectra were recorded using a Diamond ATR (attenuated total reflection) accessory (Golden Gate) at room temperature.

MOF 9

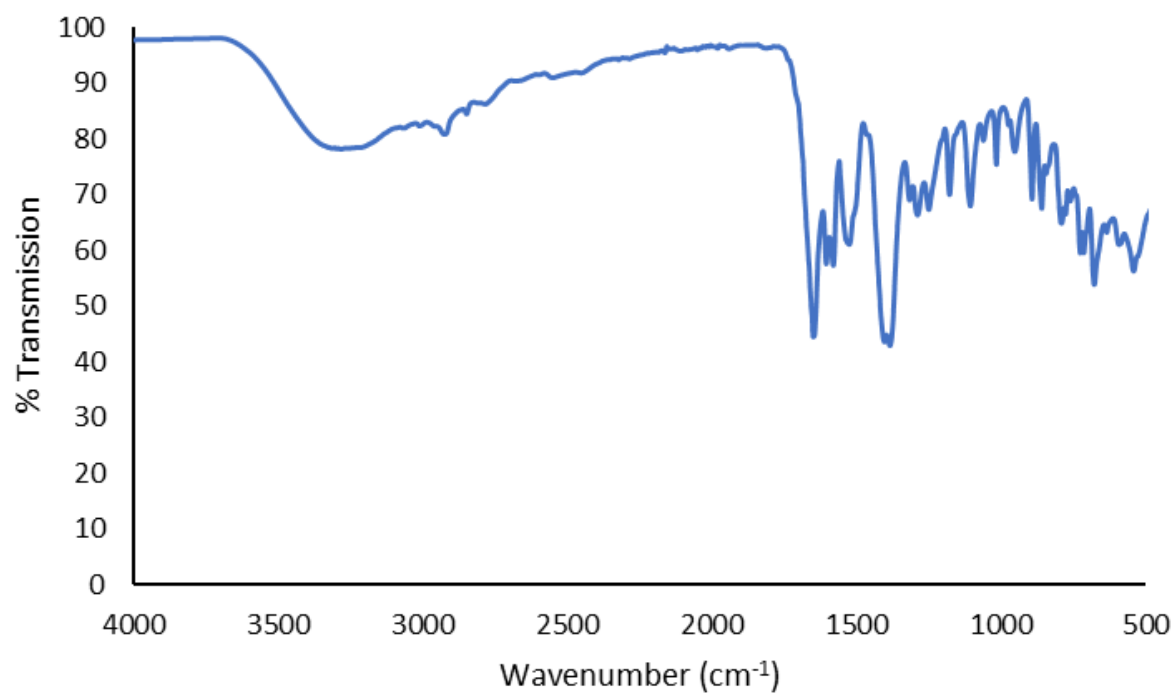


Figure S9: FTIR data for MOF 9. Infrared spectra were recorded using a Diamond ATR (attenuated total reflection) accessory (Golden Gate) at room temperature.

MOF 10

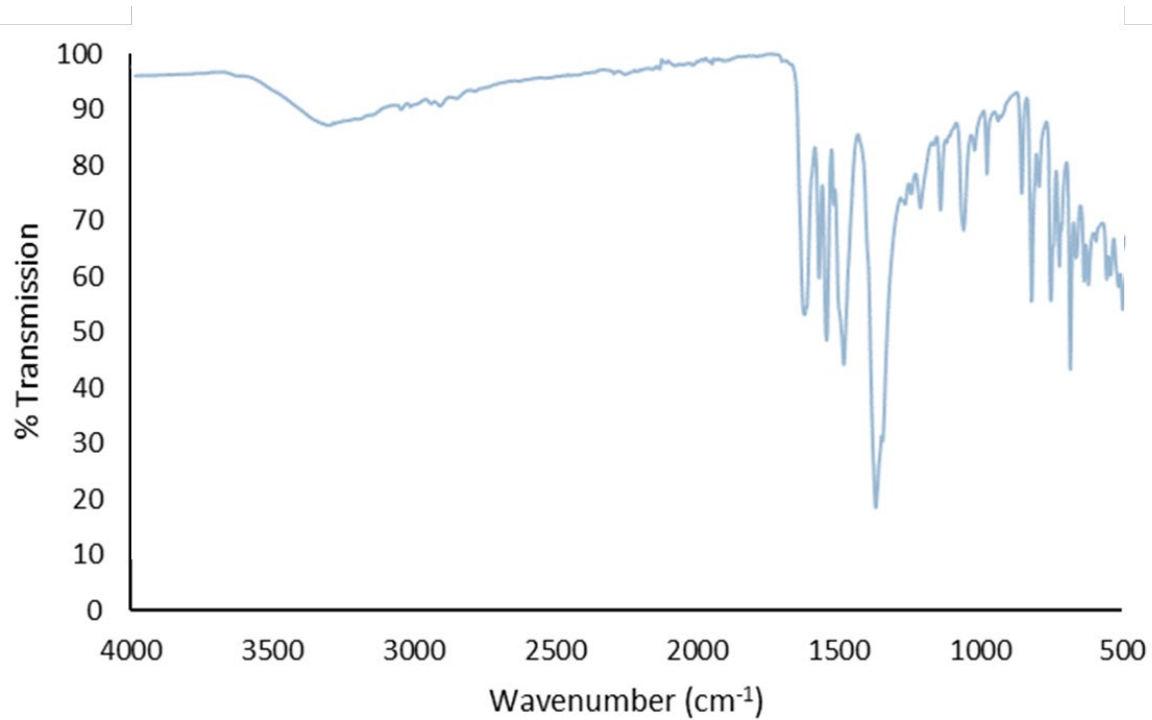
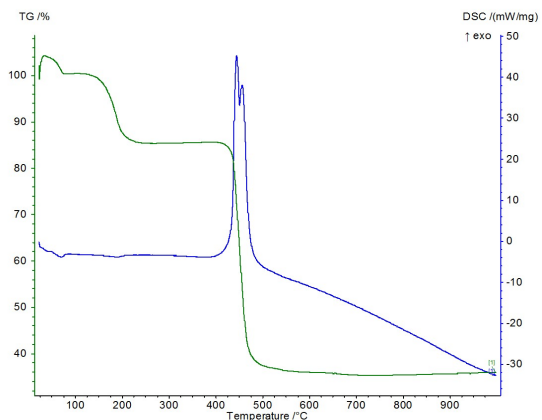


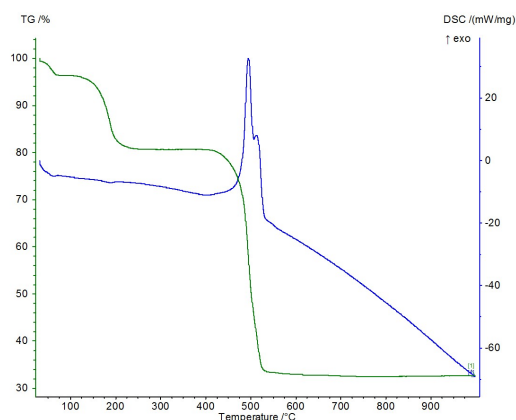
Figure S10: FTIR data for MOF 10. Infrared spectra were recorded using a Diamond ATR (attenuated total reflection) accessory (Golden Gate) at room temperature.

4. TGA and DSC data

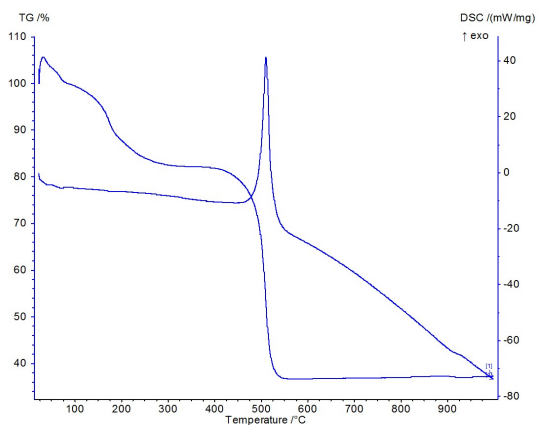
MOF 6



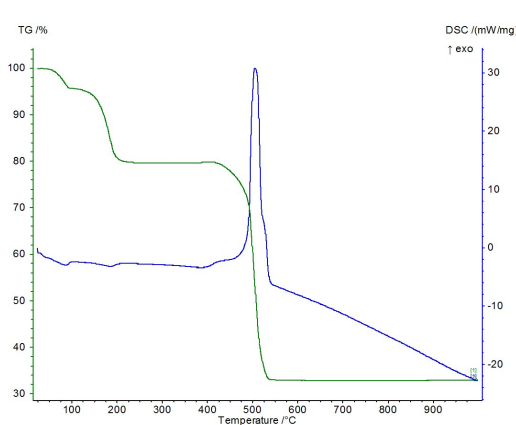
MOF 7



MOF 8



MOF 9



MOF 10

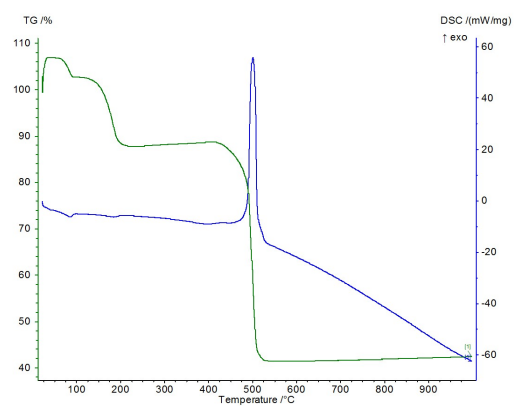


Figure S12: Thermogravimetric analysis and differential scanning calorimetry data for coordination polymers MOFs 6 - 10. Thermogravimetric analysis (TGA) was performed using Netzsch STA Jupiter simultaneous TGA-DSC system, heating rate 10°C per minute.

The appearance of initial mass gain on heating is an artifact of the buoyancy effect caused by change in the density of the carrier gas on initial heating. The average weight loss of DMF solvent molecules is 15% in figure S12, this equates for three solvent molecules at 219 g/mol.

5. PXRD Data

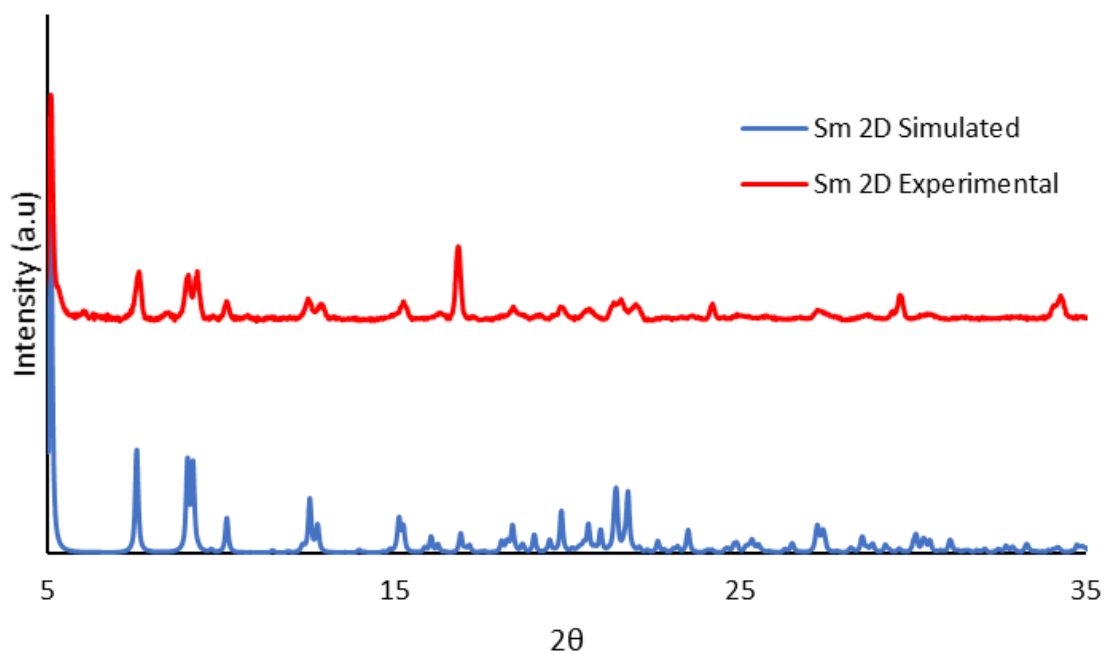


Figure S13: PXRD patterns for CP 1. Simulated pattern from single crystal data in blue vs experimental data in red. Powder X-ray diffraction (PXRD) measurements were conducted using a Rigaku XtaLAB Synergy with Cu K α radiation

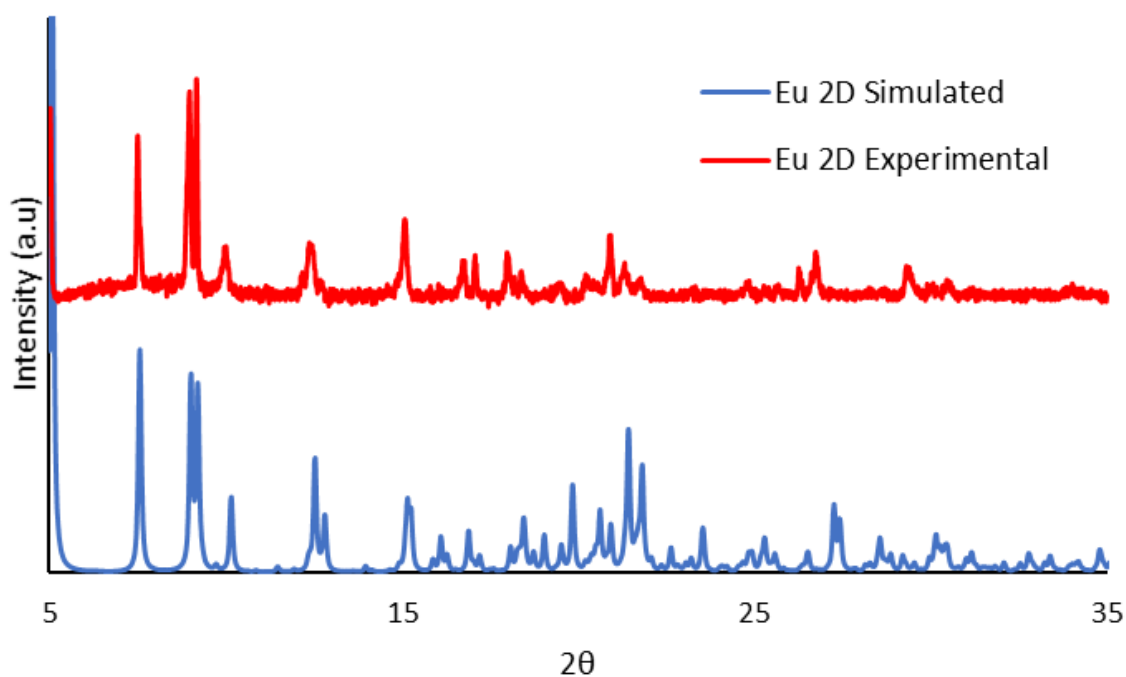


Figure S14: PXRD patterns for CP 2. Simulated pattern from single crystal data in blue vs experimental data in red. Powder X-ray diffraction (PXRD) measurements were conducted using a Rigaku XtaLAB Synergy with Cu K α radiation

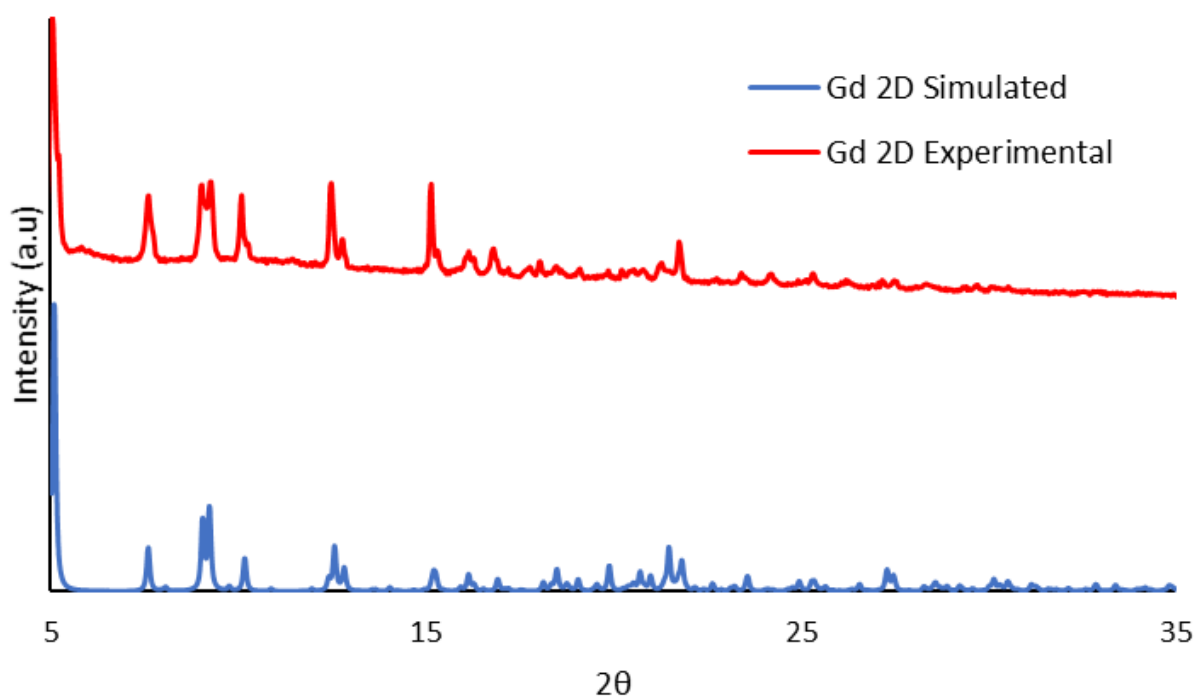


Figure S15: SPXRD patterns for CP 3. Simulated pattern from single crystal data in blue vs experimental data in red. Powder X-ray diffraction (PXRD) measurements were conducted using a Rigaku XtaLAB Synergy with Cu K α radiation

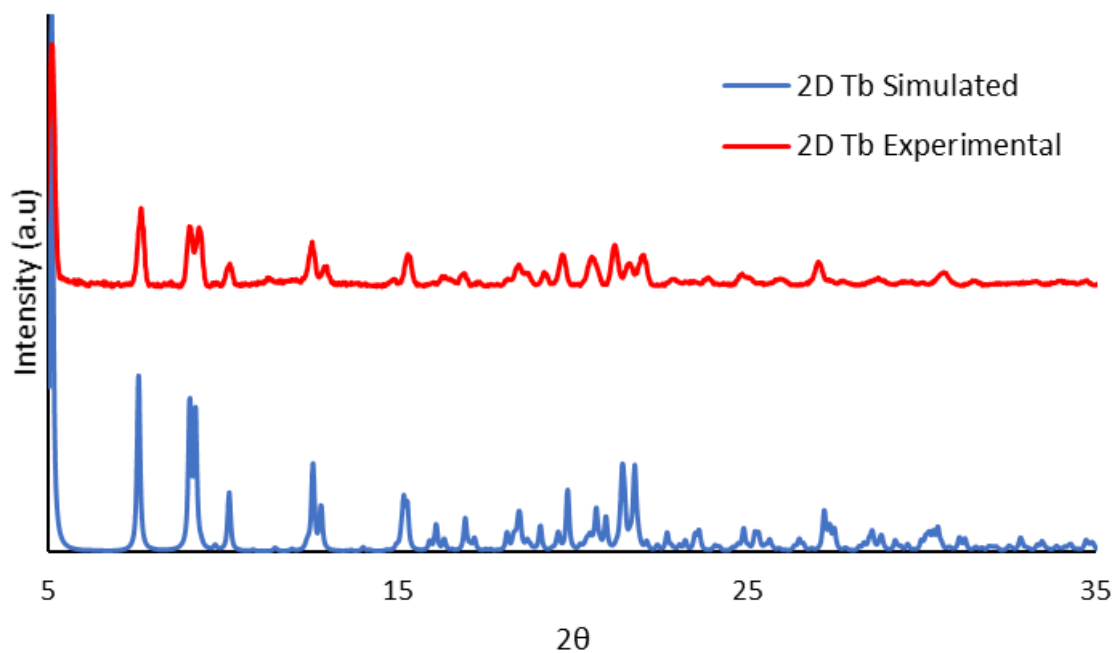


Figure S16: SPXRD patterns for CP 4. Simulated pattern from single crystal data in blue vs experimental data in red. Powder X-ray diffraction (PXRD) measurements were conducted using a Rigaku XtaLAB Synergy with Cu K α radiation

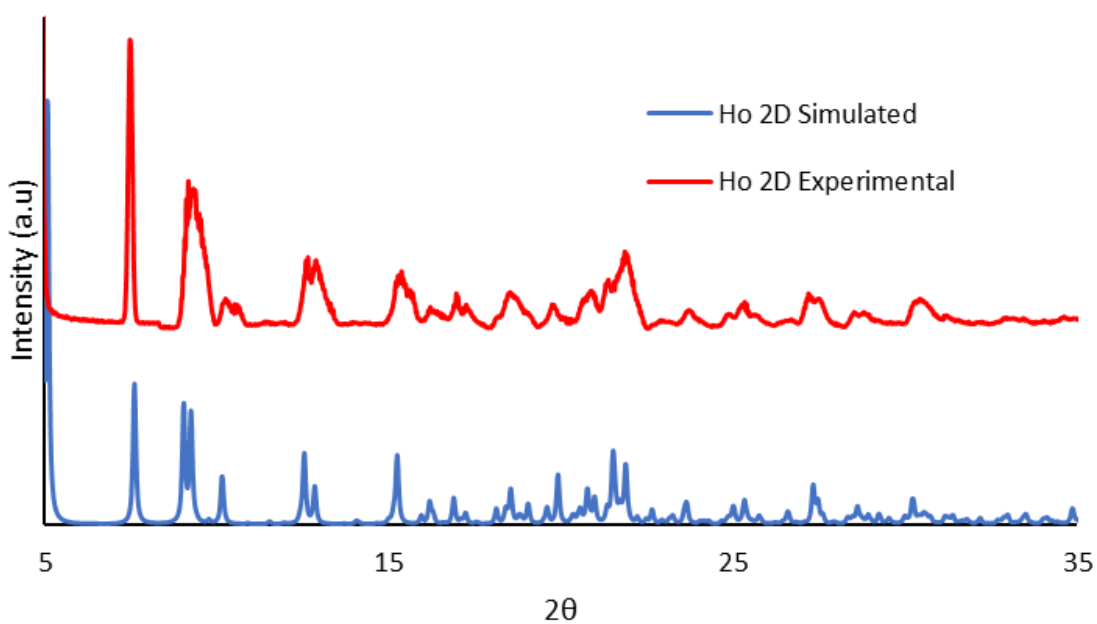


Figure S17: SPXRD patterns for CP 5. Simulated pattern from single crystal data in blue vs experimental data in red. Powder X-ray diffraction (PXRD) measurements were conducted using a Rigaku XtaLAB Synergy with Cu K α radiation

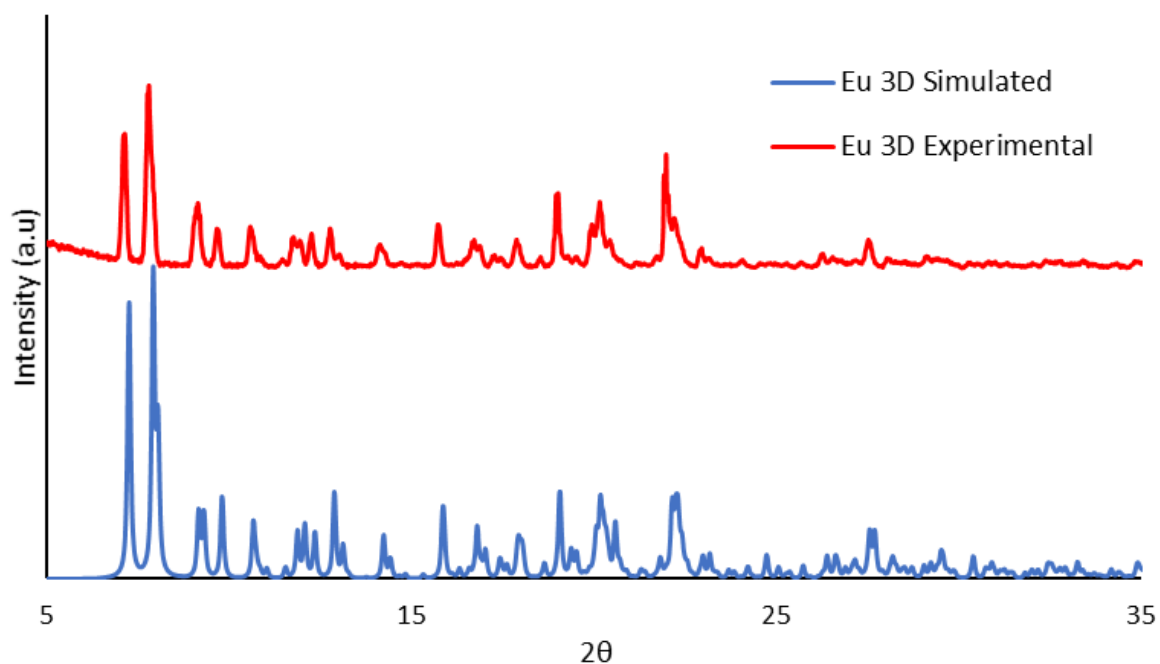


Figure S18: PXRD patterns for MOF 6. Simulated pattern from single crystal data in blue vs experimental data in red. Powder X-ray diffraction (PXRD) measurements were conducted using a Rigaku XtaLAB Synergy with Cu K α radiation

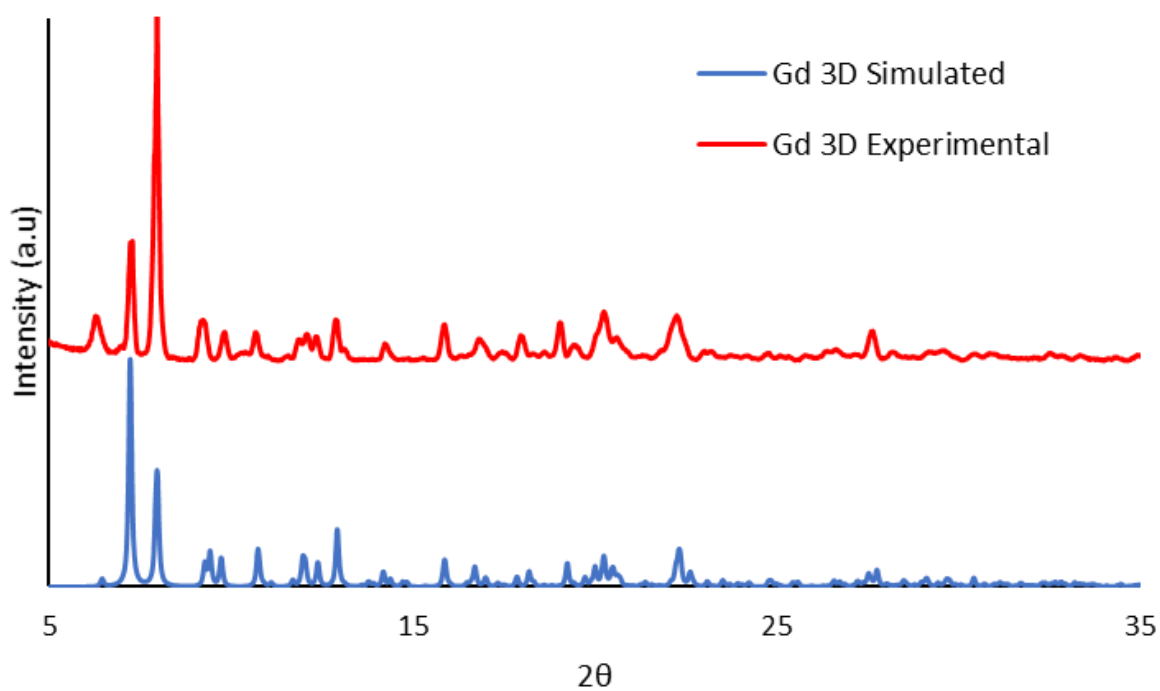


Figure S19: PXRD patterns for MOF 7. Simulated pattern from single crystal data in blue vs experimental data in red. Powder X-ray diffraction (PXRD) measurements were conducted using a Rigaku XtaLAB Synergy with Cu K α radiation

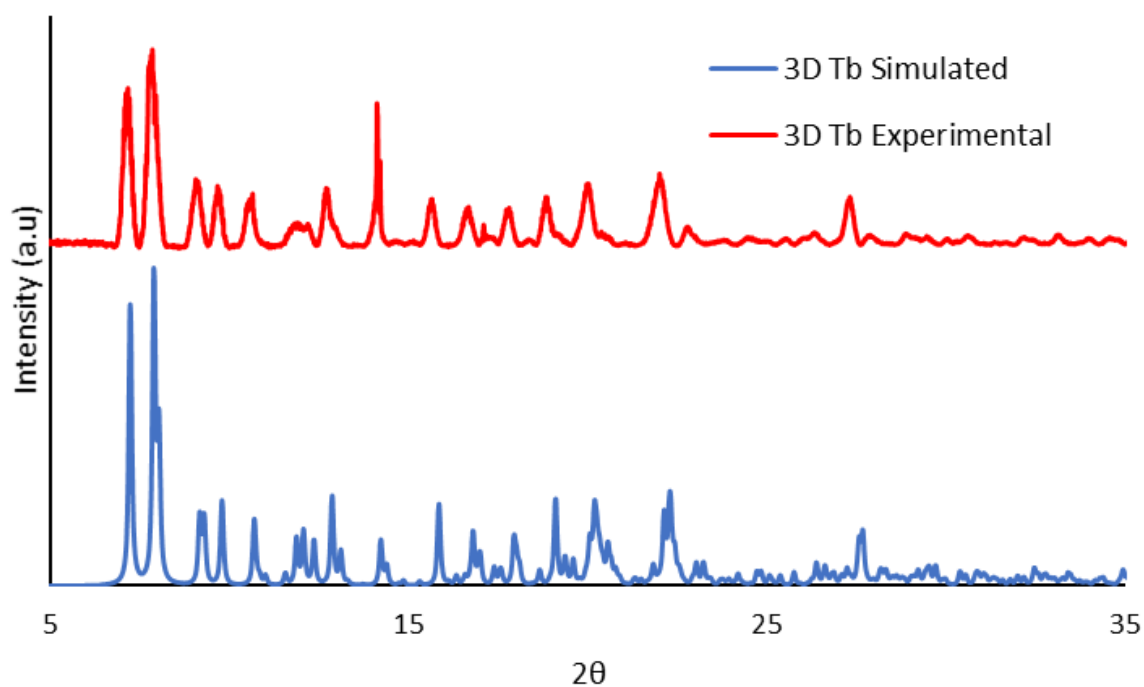


Figure S20: PXRD patterns for MOF 8. Simulated pattern from single crystal data in blue vs experimental data in red. Powder X-ray diffraction (PXRD) measurements were conducted using a Rigaku XtaLAB Synergy with Cu K α radiation

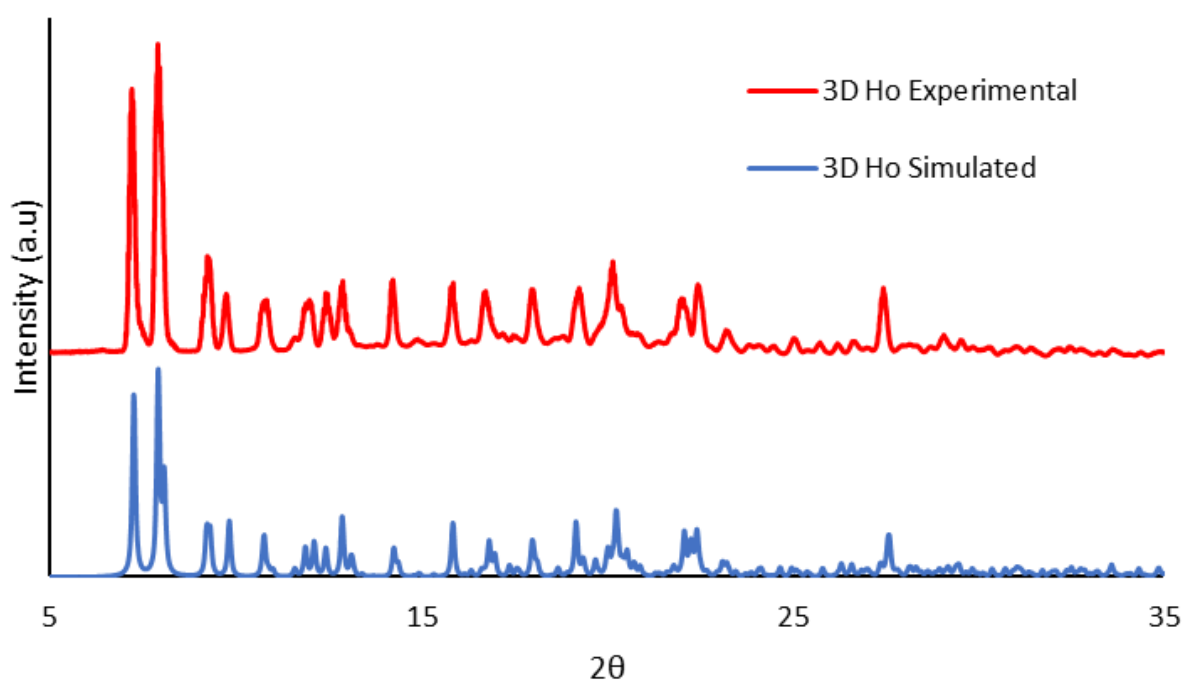


Figure S21: PXRD patterns for MOF 9. Simulated pattern from single crystal data in blue vs experimental data in red. Powder X-ray diffraction (PXRD) measurements were conducted using a Rigaku XtaLAB Synergy with Cu K α radiation

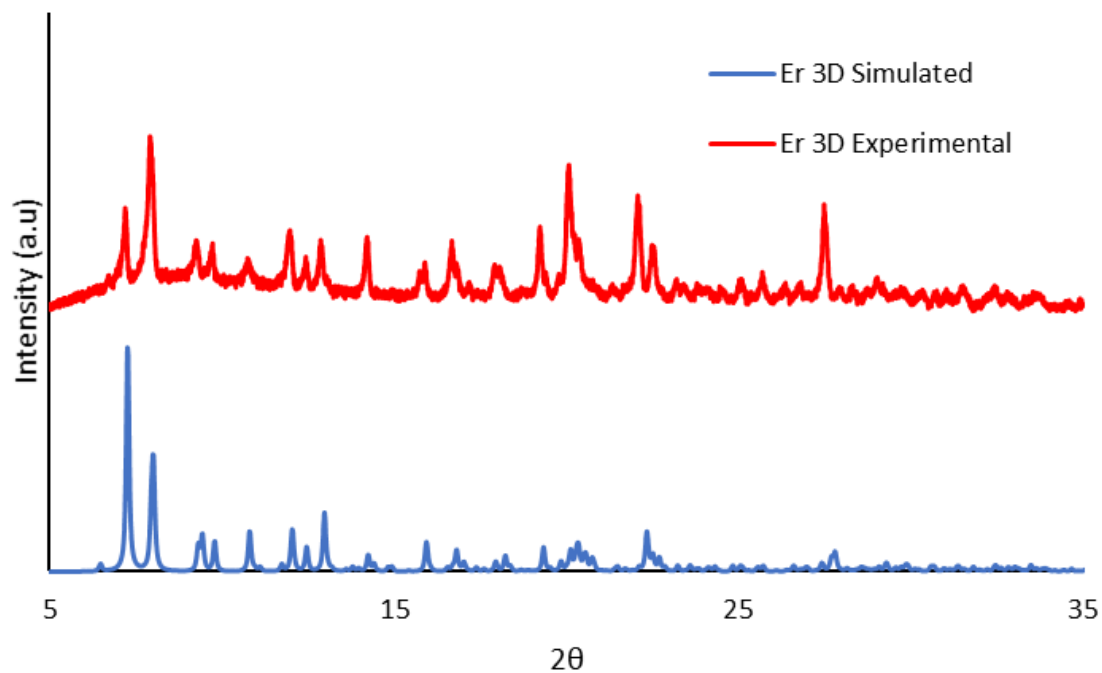


Figure S22: PXRD patterns for MOF 10. Simulated pattern from single crystal data in blue vs experimental data in red. Powder X-ray diffraction (PXRD) measurements were conducted using a Rigaku XtaLAB Synergy with Cu K α radiation

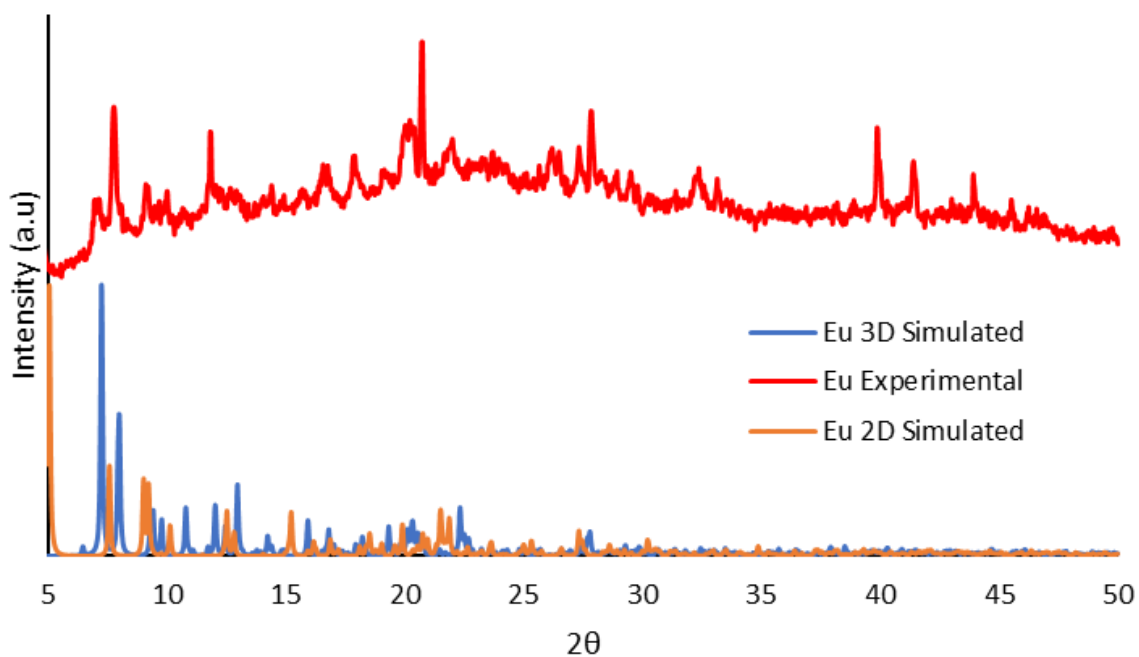


Figure S23: An example PXRD the bulk sample of Eu crystals when taken at an intermediate timeframe. Powder X-ray diffraction (PXRD) measurements were conducted using a Rigaku XtaLAB Synergy with Cu K α radiation

6. Luminescence

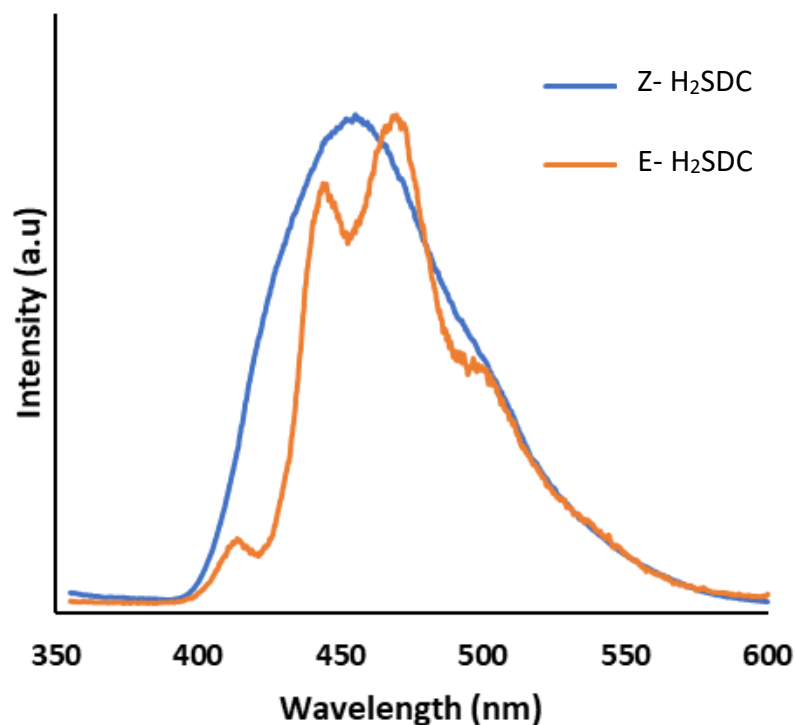


Figure S24: Luminescence spectra of *E* and *Z*-H₂SDC measured at room temperature using a Hitachi F-4500.

The control experiments revealed (*E*)-H₂SDC emission has a well-resolved structure with 2 vibronic peaks visible and a peak maxima centred at 470 nm. For (*Z*)-H₂SDC a broader more featureless emission profile is observed. Emission profiles of all frameworks show ligand-based luminescence emitted between 350-500 nm in the blue region of the electromagnetic spectrum, with the peak maxima attributed to π - π^* transitions in the highly conjugated linker in all cases.

References

- 1 AXS Bruker, Bruker AXS Inc. Madison, 2016, WI, USA
- 2 Dolomanov, O. V.; Bourhis, L. J.; Gildea, R. J.; Howard, J. A. K.; Puschmann, H. OLEX2: A Complete Structure Solution, Refinement and Analysis Program. *J. Appl. Crystallogr.* 2009, 42 (2), 339–341.
- 3 G. M. Sheldrick, *Acta Crystallogr. Sect. C Struct. Chem.*, 2015, **71**, 3–8.
- 4 G. M. Sheldrick, *Acta Crystallogr. Sect. A Found. Crystallogr.*, 2008, **64**, 112–122.
- 5 CrysAlisPro, Rigaku Oxford Diffraction, Tokyo, Japan.